Phytopathology Research

RESEARCH

Open Access

Systemic screening of *Fusarium oxysporum* candidate effectors reveals FoSSP17 that suppresses plant immunity and contributes to virulence

Tian Wang[1,2], Yun Xu[1,2], Yang Zhao[1,2], Xiaofei Liang[3], Shuang Liu[1,2], Yufang Zhang[1,2], Zhensheng Kang[3], Daipeng Chen[1,2*] and Li Zheng[1,2*]

Abstract

Fusarium oxysporum f. sp. *cubense* (*Foc*) causes Fusarium wilt of banana (*Musa* spp.), a notorious soil-borne vascular fungal disease threatening the global banana industry. Phytopathogens secrete effectors to suppress plant immunity. However, little is known about the effectors of *Foc* race 4 (*Foc4*). In this study, we built a streamlined screening system (candidate effector prediction, RNA-seq-based expression level analysis, and cell death manipulative activity assessment based on transient expression in *Nicotiana benthamiana*) to identify candidate virulence-related effectors. In total, 80 candidate effector genes (CEGs) differentially expressed during plant colonization were predicted; 12 out of 15 characterized CEGs, including *FoSSP17*, could suppress BAX-triggered programmed cell death (PCD) in *N. benthamiana* and were induced during the infection of plants. *FoSSP17* encodes a novel protein conserved in the *Fusarium* genus. *FoSSP17* gene deletion mutants were not affected in vegetative growth and conidiation but showed reduced virulence. Furthermore, the deletion mutants triggered higher expression levels of host defense-related genes including *PR1, PR3, PR5*, and *PR10*. Signal peptide activity assay and subcellular localization assay suggested that FoSSP17 is a conventional secretory protein that exerts cell-death-suppressive activity inside plant cells. In addition, FoSSP17 suppressed pattern-triggered immunity in plants by inhibiting reactive oxygen species (ROS) accumulation, reducing callose deposition, and suppressing the expression of *NbLOX* and *NbERF1* genes related to jasmonic acid (JA)-pathway and ethylene (ET)-pathway, respectively. Overall, a systemic screening of *Foc4* candidate effectors reveals that FoSSP17 contributes to the virulence of *Foc4* and suppresses pattern-triggered immunity in plants.

Keywords *Fusarium oxysporum* f. sp. *cubense*, Effector, Plant innate immunity, Virulence, Cell death

*Correspondence:
Daipeng Chen
chen.daipeng@163.com
Li Zheng
zhenglihappy0617@126.com
Full list of author information is available at the end of the article

Background

In nature, plants evolve an immune system with common features of vertebrates' innate immunity to defend against potential microbial attacks (Ausubel 2005; Chisholm et al. 2006). The plant immune system contains two overlapping layers, summarized as a 'Zigzag' model (Jones and Dangl 2006). In the first layer of immunity, pathogen-associated or microbe-associated molecular patterns (PAMPs or MAMPs) are recognized by pattern recognition receptors (PRRs) on the plant cell surface, and the triggered immune response is called PAMP-triggered immunity (PTI) (Dubery et al. 2012). Adapted pathogens secrete effectors that interfere with immunity triggered by PRRs, resulting in effector-triggered susceptibility (ETS). In the second layer of immunity, some pathogen-secreted effectors are directly or indirectly recognized by the resistance (R) proteins, including the nucleotide-binding leucine-rich repeat (NLR) proteins, thereby activating the effector-triggered immunity (ETI) (Jones et al. 2016). ETI is generally an accelerated and amplified PTI response that typically leads to localized cell death, known as the hypersensitive response (HR) (Newman et al. 2013).

Plant pathogens, such as *Fusarium oxysporum* f. sp. *cubense* (*Foc*), the causal agent of Fusarium wilt of banana (*Musa* spp.), damage global banana production. Fusarium wilt of banana was first reported in Australia in 1874. *Foc* can be divided into four physiological races (*Foc1*, *2*, *3*, and *4*) based on their virulence variation toward host cultivars, and *Foc4* is further separated into tropical race 4 (TR4) and subtropical race 4 (STR4) (Ploetz 2015a). *Foc1* and *Foc4* are economically important. *Foc1* is pathogenic to Gros Michel varieties and attacks banana triploid *Musa* AAA and *Musa* AAB (Ploetz , 2006). Compared with STR4, *Foc* TR4 is more virulent, which affects important banana cultivars in the Cavendish subgroup (Ploetz 2015b).

Foc is a soil-borne fungus with a hemibiotrophic lifestyle during the infection of plants. The conidia and hyphae of *Foc* invade host roots, and then the infectious hyphae penetrate the xylem tissue and reach pseudostem before switching to a necrotrophic stage, resulting in leaf yellowing and even plant death (Dita et al. 2018). Identifying virulence genes in *Foc* is essential in understanding pathogenic mechanisms and engineering host resistance. Effectors are fundamental to the virulence of *Foc* (Meldrum et al. 2012). Still, only a few virulence-related effectors have been identified in *Foc* so far, including homologs of SIX (secreted-in-xylem) proteins, first identified in *Fusarium oxysporum* f. sp. *lycopersici* (*Fol*) (Rep et al. 2004). Among them, Focub-SIX1a and SIX8 contribute to the virulence of *Foc* TR4 (Widinugraheni et al. 2018; An et al. 2019). *FocSge1*, a gene conserved in race 1 and race 4, regulates the expression of effector genes (Gurdaswani et al. 2020). Since high-quality genomic data are available for *Foc* (Guo et al. 2014), a large number of candidate effector genes (CEGs) have been predicted in *Foc* TR4 using genome sequencing and bioinformatics (data not published) (Zhang et al. 2021). However, the virulence functions of many of these CEGs are unrecognized. Therefore, the screening and virulence analysis of CEGs is critical for studying the host–pathogen interaction.

Transient expression of candidate effectors (CEs) in *Nicotiana benthamiana* is widely used to characterize the function of CEs of various pathogens (Wang et al. 2011). BAX, a death-promoting protein of the Bcl-2 family, is usually used as a positive control for assessing the PCD-manipulative activity of CEs (Lacomme and Santa 1999; Jamir et al. 2004). This strategy has uncovered various virulence effectors such as CfEC92, INF1, and PvRXLR159 (Kamoun et al. 1998; Lei et al. 2019; Shang et al. 2020), and 17 PvRxLR CEs strongly suppressing BAX- and INF1-triggered PCDs have been identified from *Plasmopara viticola* (Xiang et al. 2016).

This study combined bioinformatic prediction, transcriptomic analysis, transient expression in *N. benthamiana*, and loss-of-function assay to identify the *Foc4* virulence effectors. Based on this system, we identified a candidate effector gene *FoSSP17* encoding a novel small secreted protein, which could suppress BAX-triggered PCD when over-expressed in *N. benthamiana*. We showed that *FoSSP17* is conserved in the *Fusarium* genus, and its expression was up-regulated during plant infection. Additionally, we showed that FoSSP17 could suppress pattern-triggered immunity in *N. benthamiana* by reducing ROS accumulation and callose deposition. Moreover, we demonstrated the role of FoSSP17 in virulence by gene deletion and complementation assay. Collectively, our study identifies a novel protein, FoSSP17, which could suppress pattern-triggered immunity in plants to promote the *Foc4* infection.

Results

Multiple screening revealed 12 CEGs in *Foc4* with cell death manipulative activity

Candidate effectors were predicted from the annotated proteome of *Foc4* (14,932 proteins) based on an analysis pipeline encompassing SignalP5.0, TMHMM, and EffectorP3.0 predictions (Additional file 1: Figure S1). In total, 428 candidate effectors were obtained. To investigate the expression dynamics of these candidate effectors during the infection process, we conducted RNA-seq analysis with five sample types (three replicates each) representing conidia (CON), vegetative hyphae (HYP), and banana root infected by *Foc4* for 24 h (IR24), 48 h (IR48), and

72 h (IR72). Samples were sequenced with the Illumina sequencing platform, and 791.1 million raw reads and 118.7 Gb raw data were generated. The 15 RNA-seq libraries formed sample type-defined clusters in the hierarchical heatmap, indicating that gene expression levels had low biological variability within the same treatment conditions (Additional file 1: Figure S2a). A total of 4,157 differentially expressed genes (DEGs) were identified with a combination of DESeq2 and edgeR programs, and these DEGs showed at least a 4-fold expression difference in at least one of the ten pairwise comparisons. Hierarchical clustering of DEGs based on FPKM profiles was presented as a heatmap (Additional file 1: Figure S2b). Among the 428 effector repertoire, 80 genes were defined as CEGs for showing significantly up-regulated expression during infection (Additional file 2: Table S1).

Next, we used the transient expression system of *N. benthamiana* to dissect the function of CEGs. We randomly selected 20 CEGs to test the PCD-suppressive activity, and 15 genes were successfully cloned into the potato virus X (PVX) vector pGR107. We observed that only one clone, *FoSSP1*, triggered PCD at 5 d post-inoculation (Wang et al. 2022), 2 had no activity, and 12 suppressed BAX triggered-PCD when injected 24 h before BAX (Table 1 and Additional file 1: Figure S3). To determine the expression dynamics of the 12 candidate effectors, the relative expression levels of these genes were quantified by qRT-PCR. Compared with 0 h post-inoculation (hpi), all 12 genes showed significant up-regulation at 12, 24, 48, or 72 hpi (Additional file 1: Figure S4), which is in accordance with the transcriptome analysis results. These results suggested that the 12 candidate effectors may function during the plant infection stage.

FoSSP17 is conserved in the *Fusarium* genus

We randomly selected 3 (*FoSSP17*, *FoSSP20*, and *FoSSP48*) cell-death-suppressing CEGs for further characterization. *FoSSP17* (FOIG_10239; Gene ID: 42035414; NCBI Reference Protein Sequence: XP_031060038.1) encodes a hypothetical protein with 172 amino acids. The protein was predicted to contain an N-terminal signal peptide (SP) and no transmembrane domain (TMD). To determine the phylogenetic distribution of FoSSP17 homologs, BlastP searches against the National Center for Biotechnology Information (NCBI) non-redundant (NR) database and the Ensemble Fungi database were conducted. A large number of homologs from various *Fusarium* strains were identified with amino acid identity over 57.31% (Fig. 1a). Interestingly, homologs were also found in other Ascomycetes, and all belong to the Hypocreomycetidae subclass. Sequence analysis using Clustal W revealed homologs of FoSSP17 with high identity (Fig. 1b). These results indicate that FoSSP17 homologs distribute widely in the Hypocreomycetidae subclass while are more conserved in the *Fusarium* genus.

FoSSP17 is a conventional secretory effector that exerts cell-death-suppressive activity inside plant cells

Bioinformatics analysis suggested that FoSSP17 contains an N-terminal SP. We used the yeast secretion system

Table 1 Characteristics of 15 candidate effectors from *Foc4*

Candidate effector	Gene ID	Length	Description	Induce PCD or suppress BAX-triggered PCD
FoSSP1	FOIG_06406	145	Uncharacterized protein	Induce
FoSSP16	FOIG_10132	185	Uncharacterized protein	Suppress
FoSSP17	FOIG_10239	172	Uncharacterized protein	Suppress
FoSSP20	FOIG_10940	82	Uncharacterized protein	Suppress
FoSSP25	FOIG_11731	186	Uncharacterized protein	Suppress
FoSSP31	FOIG_13546	232	Uncharacterized protein	Suppress
FoSSP40	FOIG_14677	310	Uncharacterized protein	Suppress
FoSSP45	FOIG_14845	166	Uncharacterized protein	Suppress
FoSSP48	FOIG_15139	111	Uncharacterized protein	Suppress
FoSSP49	FOIG_15140	152	Uncharacterized protein	No effect
FoSSP54	FOIG_15739	260	Uncharacterized protein	Suppress
FoSSP55	FOIG_16626	128	Uncharacterized protein	Suppress
FoSSP69	FOIG_03936	375	Uncharacterized protein	No effect
FoSSP71	FOIG_04289	239	Uncharacterized protein	Suppress
FoSSP80	FOIG_06254	339	Uncharacterized protein	Suppress

Induce: CEs could induce PCD in *N. benthamiana*; Suppress: CEs could suppress BAX-triggered PCD in *N. benthamiana;* No effect: CEs can neither suppress BAX-triggered PCD nor induce PCD in *N. benthamiana*

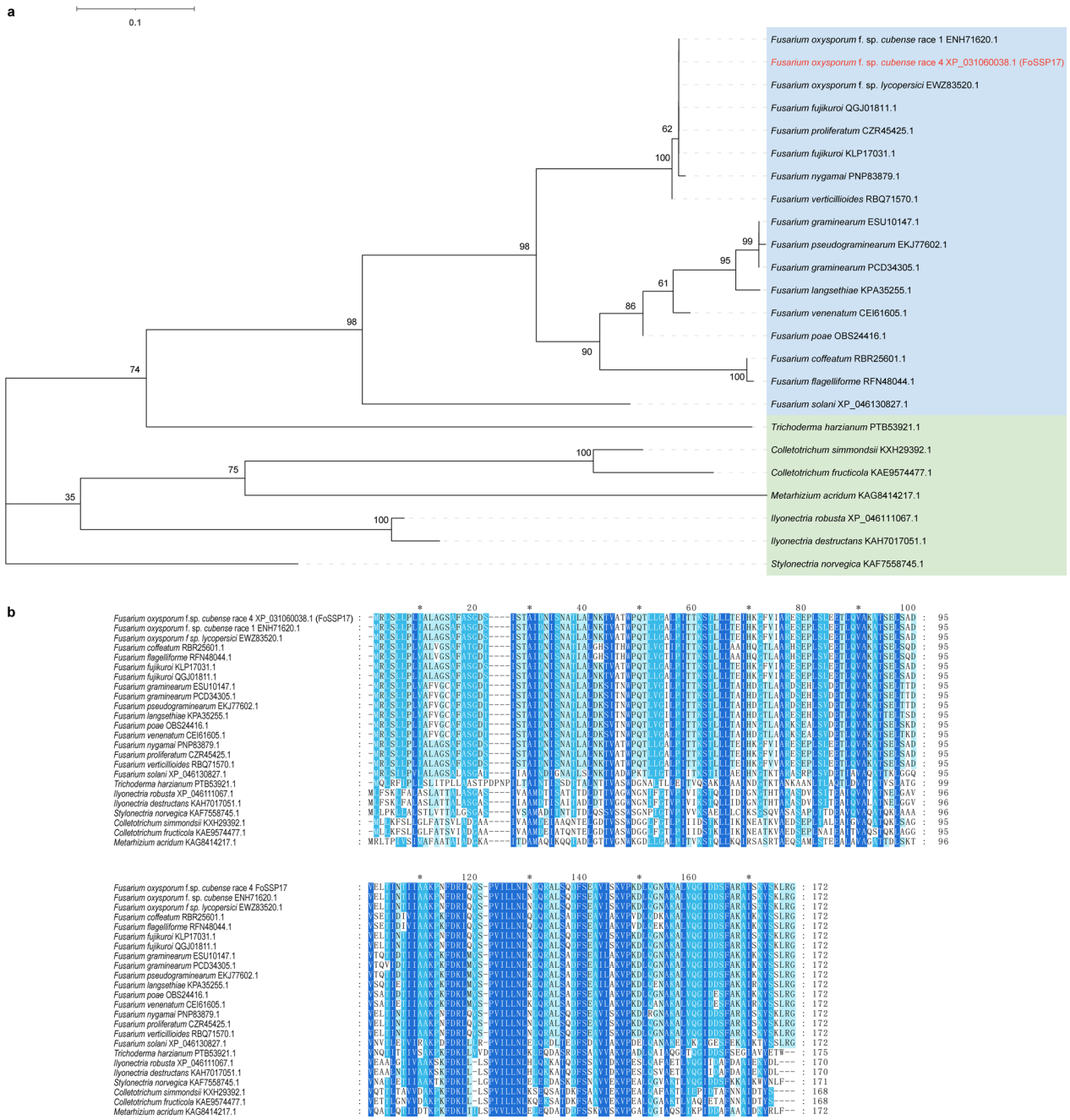

Fig. 1 FoSSP17 homologs are widely distributed in the Hypocreomycetidae subclass. **a** The phylogeny of FoSSP17 and its homologous sequences from selected species. The tree was constructed by MEGA11 using the maximum-likelihood method. Bootstrap percentage support for each branch is indicated (1000 replication). The scale bar corresponds to a genetic distance of 0.01. Sequences from *Fusarium* and other Hypocreomycetidae species are marked with a light blue and green background, respectively. **b** Amino acid alignment of FoSSP17 and its homologous proteins. Clustal W was used to align all protein sequences, and the alignment was edited by GeneDoc. Conservative amino acids are shaded with a blue background, and the shading intensity indicates the level of amino acid identity

to verify the secretory function of the predicted SP (Yin et al. 2018). The full length of SP (N-terminal 17 amino acids) was successfully cloned in the pSUC2 vector and then transferred into the yeast *Saccharomyces cerevisiae* YTK12 strain. The predicted SP of FoSSP17 was sufficient to mediate the secretion of invertase enzyme in the YTK12 strain (Fig. 2a), supporting that FoSSP17 is a conventional secretory protein. We further tested whether

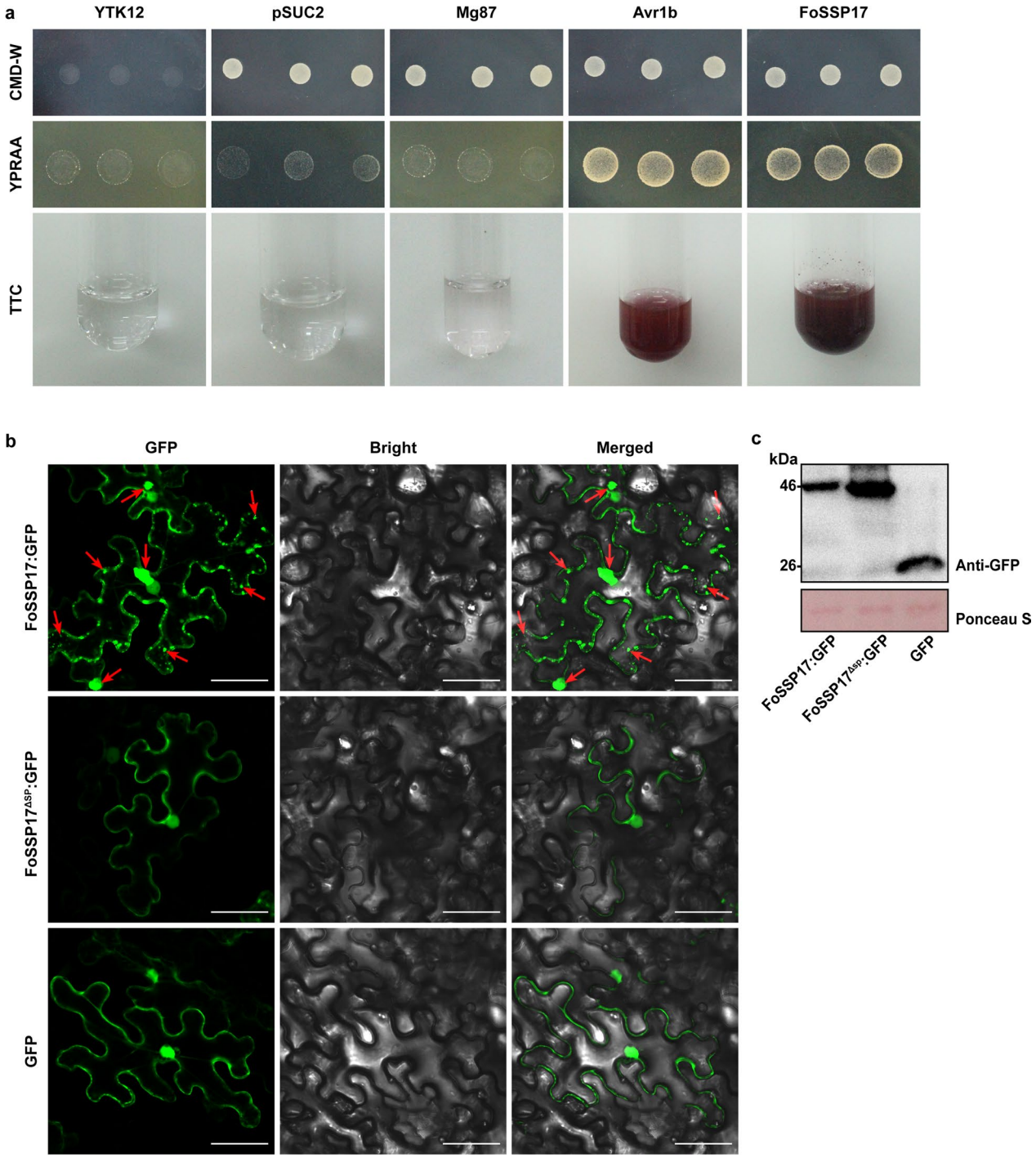

Fig. 2 Functional validation of SP of FoSSP17 and subcellular localization of FoSSP17 and FoSSP17$^{\Delta SP}$. **a** Verifying the SP function of FoSSP17 by yeast secretion system.Yeast *Saccharomyces cerevisiae* YTK12 strain and strains bearing the empty pSUC2 vector and the pSUC2 vector with the SP of Mg87 protein from *Magnaporthe oryzae* were used as negative controls; the strain harboring the pSUC2 vector with the SP of Avr1b protein from *Phytophthora sojae* was used as the positive control. **b** Subcellular localization of FoSSP17 and FoSSP17$^{\Delta SP}$. Leaves of *N. benthamiana* transiently expressing FoSSP17:eGFP and FoSSP17$^{\Delta SP}$:eGFP fusion proteins were examined by confocal microscopy. GFP was used as a control. The accumulated FoSSP17:eGFP is indicated with red arrows. Bars = 50 μm. **c** Western blot analysis of protein from *N. benthamiana* leaves expressing GFP, FoSSP17:eGFP, and FoSSP17$^{\Delta SP}$:eGFP. The same results were obtained with at least three biological replicates

the SP is important for FoSSP17's cell-death suppressive activity. FoSSP17 and FoSSP17 lacking SP (FoSSP17$^{\Delta SP}$) were cloned into the pGR107-*GFP* vector. The C-terminal GFP fusion proteins of FoSSP17 and FoSSP17$^{\Delta SP}$ were transiently expressed in *N. benthamiana*. Then, the BAX protein was transiently expressed at the same location 24 h later. Results showed that BAX strongly induced PCD at 5 d post inoculation (dpi), whereas both FoSSP17 and FoSSP17$^{\Delta SP}$ could fully suppress BAX-triggered PCD (Fig. 3a, b). The expression of FoSSP17 and FoSSP17$^{\Delta SP}$ GFP fusion proteins in the tobacco leaves was confirmed by western blot (Fig. 3c).

To overcome the host's PTI, pathogens secrete effectors that could target plant apoplast or cytoplasm, termed apoplastic and cytoplasmic effectors, respectively (Asai and Shirasu 2015). To validate the subcellular localization of FoSSP17 in plants, we infiltrated agro strains bearing pBin-*FoSSP17-eGFP* or pBin-*FoSSP17$^{\Delta SP}$-eGFP* vectors into *N. benthamiana* leaves and pBin-*eGFP* empty vector was used as a control. Confocal microscopy observation revealed that both FoSSP17:eGFP and FoSSP17$^{\Delta SP}$:eGFP localized in the nucleus and plasma membranes in *N. benthamiana* cells (Fig. 2b). Interestingly, transiently expressed FoSSP17:eGFP could aggregate as spots in the cytoplasm (Fig. 2b). Western blot analysis detected the expression of FoSSP17:eGFP and FoSSP17$^{\Delta SP}$:eGFP proteins (Fig. 2c). As a control, to clarify that FoSSP17 could be secreted in the plant, we used a functional SP from

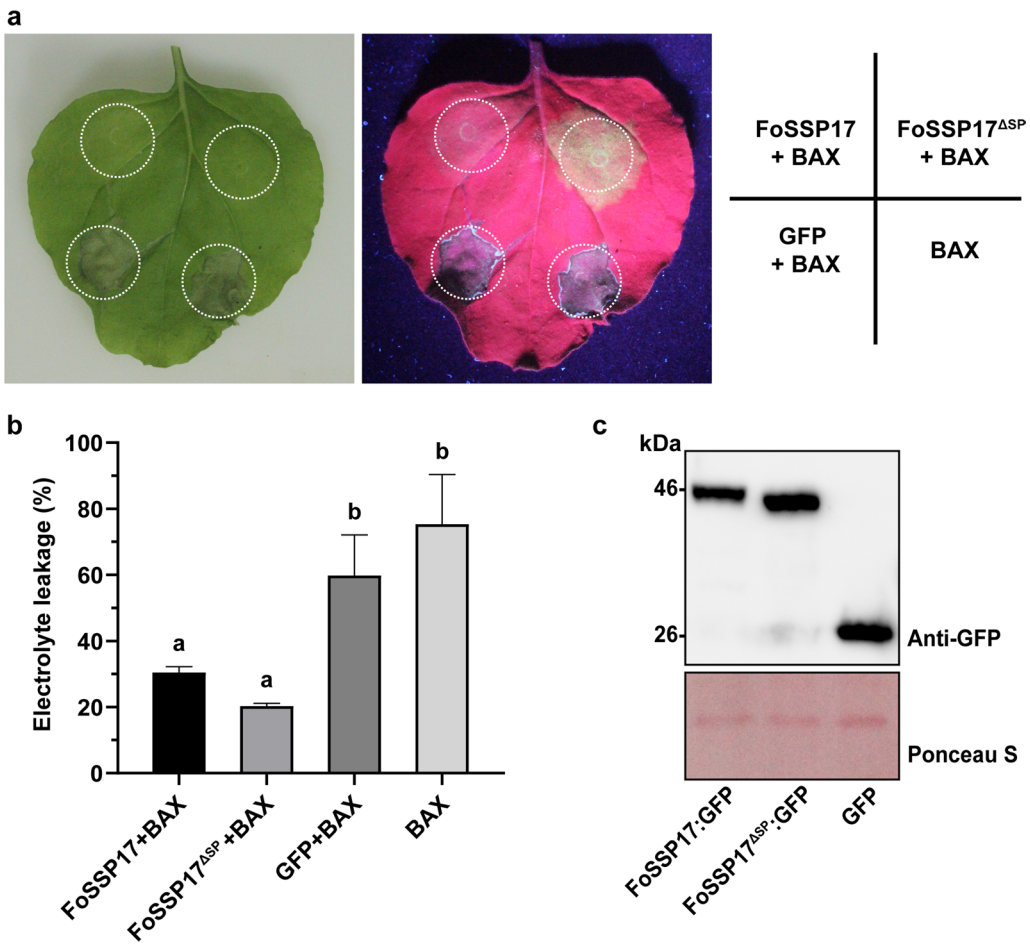

Fig. 3 Transient expression of FoSSP17 and FoSSP17$^{\Delta SP}$ in *N. benthamiana*. **a** FoSSP17 and FoSSP17$^{\Delta SP}$ suppressed BAX-induced cell death in *N. benthamiana*. Agrobacterium strains carrying pGR107-*FoSSP17-GFP*, pGR107-*FoSSP17$^{\Delta SP}$-GFP*, and pGR107-GFP (as negative control) were infiltrated separately in leaves 24 h before infiltration of the Agrobacterium expressing BAX at the same location. Dashed circles indicate the agroinfiltrated regions. Photos were taken 5 d after BAX treatment. Ultraviolet (UV) light was used to indicate the HR response. **b** Electrolyte leakage assay of *N. benthamiana* leaves co-expressing BAX with indicated proteins. Samples were collected 5 d after BAX treatment. Data shown are means ± SD calculated from three independent experiments. Statistical analyses were performed with One-way analysis of variance (ANOVA) and Tukey's multiple comparisons test. Different letters indicate significant differences ($P < 0.05$). **c** Western blot analysis of the protein expression of FoSSP17 and FoSSP17$^{\Delta SP}$ with GFP tag. Similar results were obtained from at least three biological replicates

pathogenesis-related protein 1 (PR1) to replace the original SP of FoSSP17, and constructed pBin-*FoSSP17*$^{SP(PR1)}$-*eGFP* vector (Zhang et al. 2021). In *N. benthamiana* cells transiently expressing FoSSP17$^{SP(PR1)}$:eGFP, the GFP signals of FoSSP17$^{SP(PR1)}$ accumulated mainly in the nucleus and plasma membranes (Additional file 1: Figure S5a), indicating that the SP of FoSSP17 is functional in *N. benthamiana*. Overall, these results indicate that the activity of FoSSP17 to suppress cell death in *N. benthamiana* does not depend on its SP, and FoSSP17 is targeted to the nucleus and plasma membrane of plants.

FoSSP17 suppressed pattern-triggered immunity in plants

Since FoSSP17 could suppress BAX triggered-PCD, we speculated that FoSSP17 is an effector which could suppress the plant immune responses. Plant cell-surface localized receptors could recognize MAMPs including bacterial flagellin (flg22) to induce a series of immune responses, such as ROS accumulation and callose deposition (Boller and Felix 2009). To verify our hypothesis, *A. tumefaciens* carrying pBin-*FoSSP17-eGFP* or pBin-eGFP were infiltrated in *N. benthamiana* leaves, and 20 μM flg22 was injected at the same location after 48 h. After 12 h with flg22 infiltration, the ROS accumulation was detected by staining with Diaminobenzidine (DAB), and the callose deposition was detected by aniline blue staining. The results showed that flg22 induced much lower levels of ROS accumulation and callose deposition in leaves expressing FoSSP17:GFP compared with those expressing only GFP (Fig. 4a–d). Similar results were observed when chitin elicitor (Hexa-N-acetylchitohexaose) was applied to trigger plant immunity (data not shown).

After cell-surface receptors perceive signals and activate defenses, the plant immune response is potentiated by hormone signaling pathways (Zhou and Zhang 2020). To further clarify potential mechanisms through which FoSSP17 suppresses plant immune responses, we used qRT-PCR to detect the expression levels of *PR1, PR5, PR3, LOX,* and *ERF1* genes in *N. benthamiana* after flg22 infiltration. *NbPR1* and *NbPR5* are associated with salicylic acid (SA) signaling pathway; *NbPR3* and *NbLOX* are associated with jasmonic acid (JA) signaling pathway; *NbERF1* is associated with ethylene (ET) signaling pathway (Asai and Yoshioka 2009; Ali et al. 2017, 2018). As a result, there is no significant difference in the expression levels of *NbPR1* and *NbPR5* between the tobacco leaves expressing FoSSP17:GFP and GFP. However, the expression levels of *NbPR3*, *NbLOX*, and *NbERF1* were significantly reduced in the samples expressing FoSSP17:GFP, compared with the control plants (Fig. 4e). Taken together, these results suggested that FoSSP17 manipulates pattern-triggered immunity in plants by suppressing the expression of genes involved in JA and ET signaling pathways.

FoSSP17 contributes to fungal virulence

We used the split-marker approach and protoplast transformation methods to generate the deletion mutant of *FoSSP17* (FOIG_10239) (Additional file 1: Figure S6a). Two mutants of *FoSSP17* (Δ*FoSSP17*-4 and Δ*FoSSP17*-5) harboring hygromycin resistance marker were successfully developed in *Foc4* and further confirmed by PCR (Additional file 1: Figure S6b). To complement the *FoSSP17* deletion mutant, we cloned the native promoter and coding region of *FoSSP17* into the pFL2 vector and transformed the resulting plasmid into Δ*FoSSP17* by polyethylene glycol (PEG)-mediated protoplast transformation. The genetically complemented strain (Δ*FoSSP17*-C8) was also validated by PCR (Additional file 1: Figure S6b). To investigate whether *FoSSP17* influences the vegetative growth of *Foc4*, we compared the growth rates of the wild-type (WT), deletion mutants, and the complemented strains. The results showed that mutants exhibited normal colony morphology and radial growth (Fig. 5a, b). In addition, *FoSSP17* gene deletion had no significant influence on conidiation (Fig. 5c). These results suggested that the deletion of *FoSSP17* did not affect the vegetative growth of *Foc4*.

To further investigate the role of *FoSSP17* in virulence, conidia suspension of WT, Δ*FoSSP17*-4, Δ*FoSSP17*-5, and Δ*FoSSP17*-C8 were inoculated into roots of banana plantlets separately. At 30 dpi, all inoculated plants displayed symptoms of Fusarium wilt compared with mock treatment (water-inoculated). However, the leaves, rhizomes, and corms of banana plants infected by Δ*FoSSP17*-4 and Δ*FoSSP17*-5 were healthier and had fewer necrotic lesions compared with those infected with WT and complemented strains (Fig. 6a). The disease indexes of both Δ*FoSSP17*-4 and Δ*FoSSP17*-5 decreased by approximately 20% compared with WT and the complemented strains (Fig. 6b). The reduced virulence of Δ*FoSSP17* led us to perform a qRT-PCR assay to determine the expression levels of the banana defense-related genes. Banana roots infected by WT and deletion mutants were sampled at 3 dpi for qPCR analysis of the transcript levels of the pathogenesis-related (*PR*) genes, including *PR1*, *PR3*, *PR5,* and *PR10*. Compared with WT infection, the expression levels of all *PR* genes were significantly up-regulated during Δ*FoSSP17* infection (Fig. 6c). Overall, these results support that FoSSP17 plays an essential role in the virulence of *Foc4* by suppressing host defense reactions.

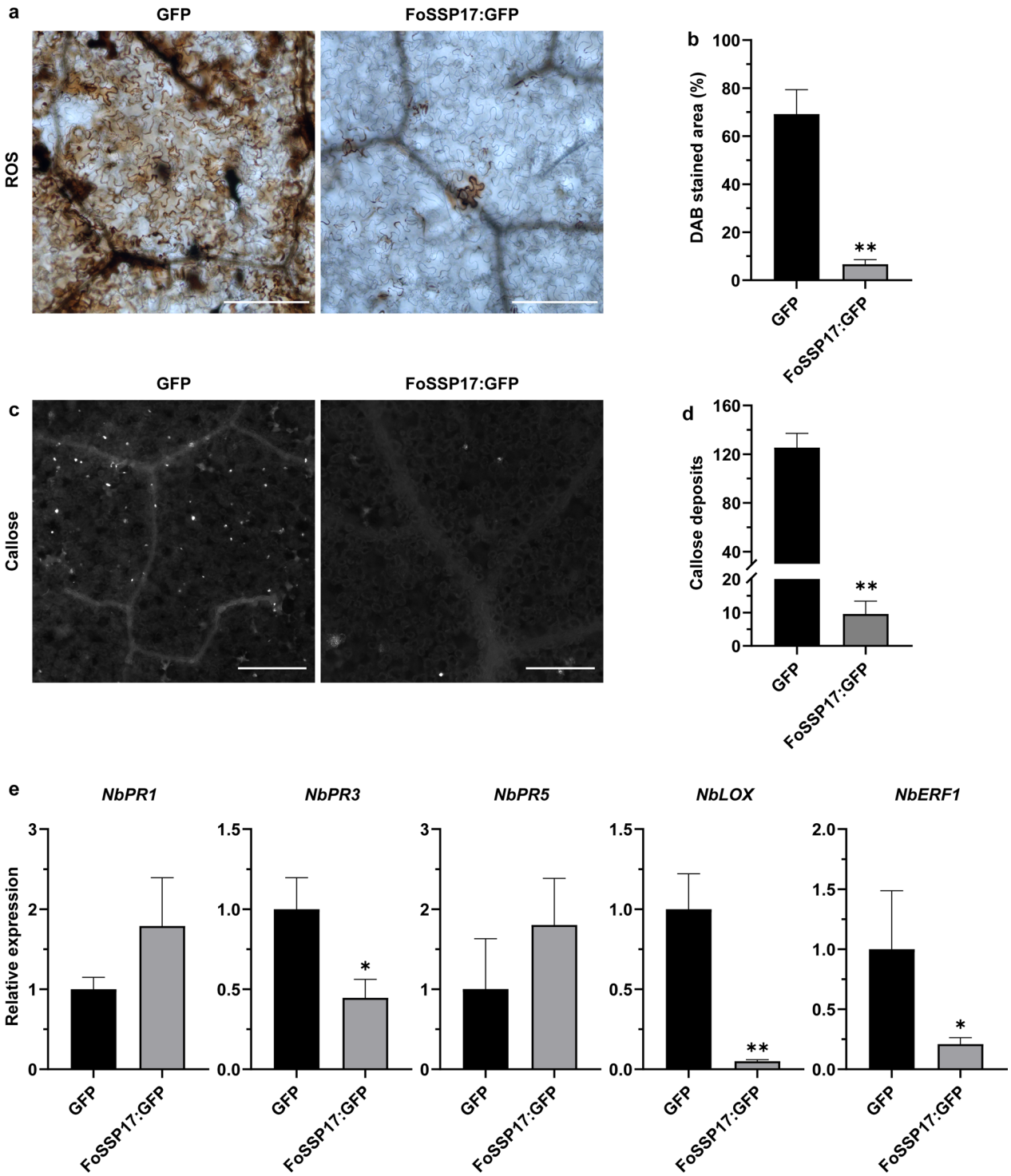

Fig. 4 FoSSP17 suppressed flg22-triggered PTI in *N. benthamiana*. **a, b** Flg22-induced ROS accumulation was suppressed in *N. benthamiana* leaves expressing FoSSP17:GFP. Samples were collected 12 h after infiltration with flg22. Photographs were taken after DAB staining (Bars = 200 μm). The relative area of DAB-stained leaf tissues was analyzed with ImageJ software. **c, d** FoSSP17:GFP suppressed flg22-induced callose deposition in tobacco leaves. Samples were collected 12 h after flg22 treatment. Photographs were taken after aniline blue staining (Bars = 200 μm). The number of callose spots per 1 mm^2 was analyzed with ImageJ software. **e** Relative transcript levels of 5 defense-related genes. Total RNA was extracted from samples collected 12 h after flg22 treatment. *NbActin* gene was used as the reference gene for normalization. Relative transcript levels of genes in leaves expressing GFP are arbitrarily set to 1. For **b**, **d**, and **e**, data shown are means ± SD calculated from three biological replicates. Statistical analyses were performed with Student's *t*-test. *$P < 0.05$; **$P < 0.01$

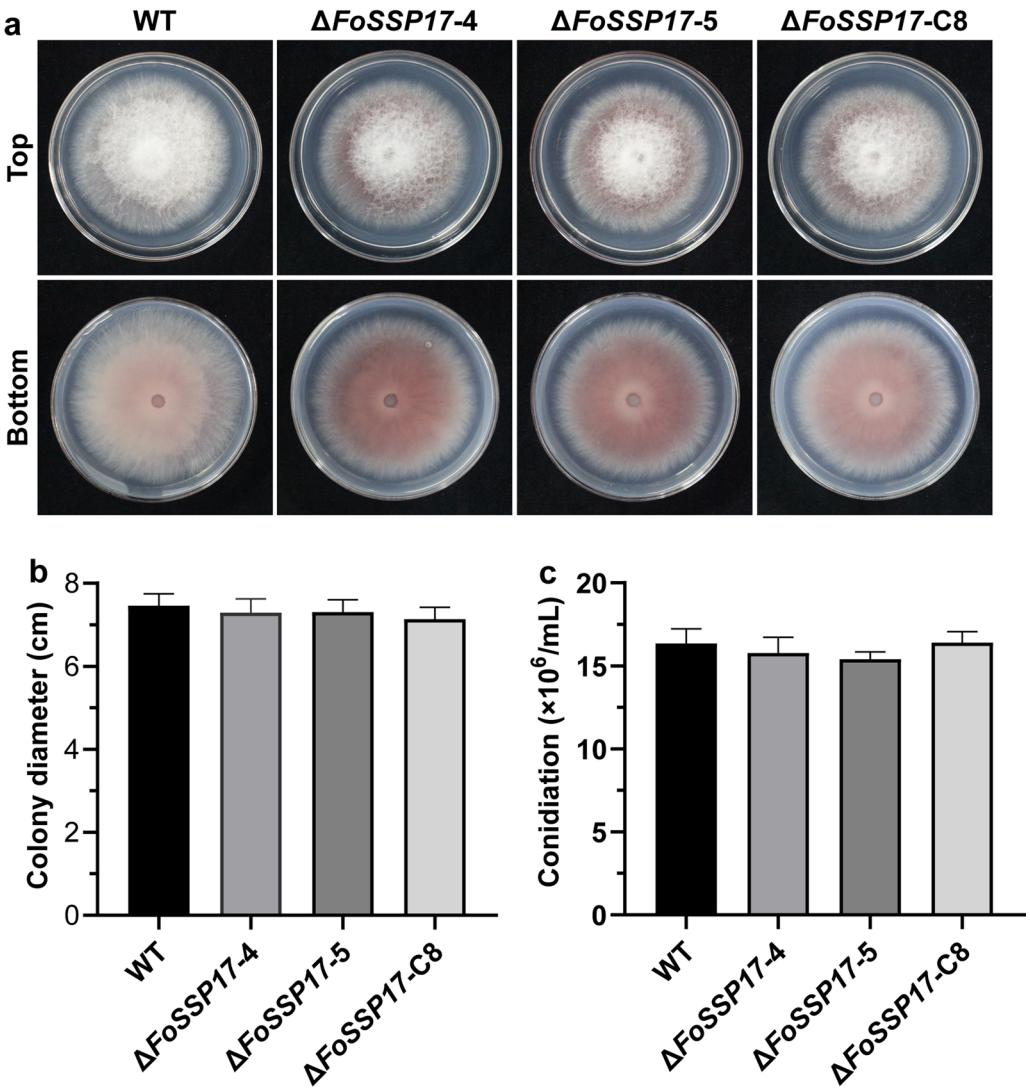

Fig. 5 *FoSSP17* gene deletion mutants are normal in colony morphology, growth rate, and conidiation. **a**, **b** Colony morphology and colony diameter of WT, deletion mutants (Δ*FoSSP17*-4 and Δ*FoSSP17*-5) and the complemented strain (Δ*FoSSP17*-C8) grown on potato dextrose agar (PDA) plates at 28°C for 6 d. **c** Conidiation of the indicated strains grown in potato dextrose broth (PDB) for 2 d. Data shown are means ± SD calculated from three biological replicates. The statistical analyses were performed with Student's *t*-test; no significant difference was found among the tested strains

Discussion

Foc4 is a soil-borne fungus that can infect banana roots and damage the banana industry (Pegg et al. 2019). *Foc4* secretes virulence factors to promote the infection process, including cell wall degrading enzymes (CWDEs), fusaric acids (FAs), and effectors (Roncero et al. 2000; López-Díaz et al. 2018). The *Foc4* secretes a large number of effectors into the host plant and manipulates plant immunity. Thus, effective screening of the *Foc4* candidate effectors is essential to clarify the pathogenic mechanisms of *Foc4*. Previous studies have used different methods to identify CEs, including yeast signal sequence trap (YSST) and bioinformatic analysis (Krijger et al. 2008; Saunders et al. 2012). Transient expression of candidate effectors in *N. benthamiana* is a powerful method to characterize CEs such as *Phytophthora sojae* RXLR effectors (Wang et al. 2011). Agro-infiltrated *N. benthamiana* leaves expressing the *Phytophthora sojae* Avr1d protein suppress BAX-triggered PCD and enhance *P. capsici* infection (Yin et al. 2013). Furthermore, transcriptome analysis of tomato plants infected by *Fol* identified 27 novel CEGs that were significantly up-regulated during the infection stage, 22 of which could suppress or induce cell death

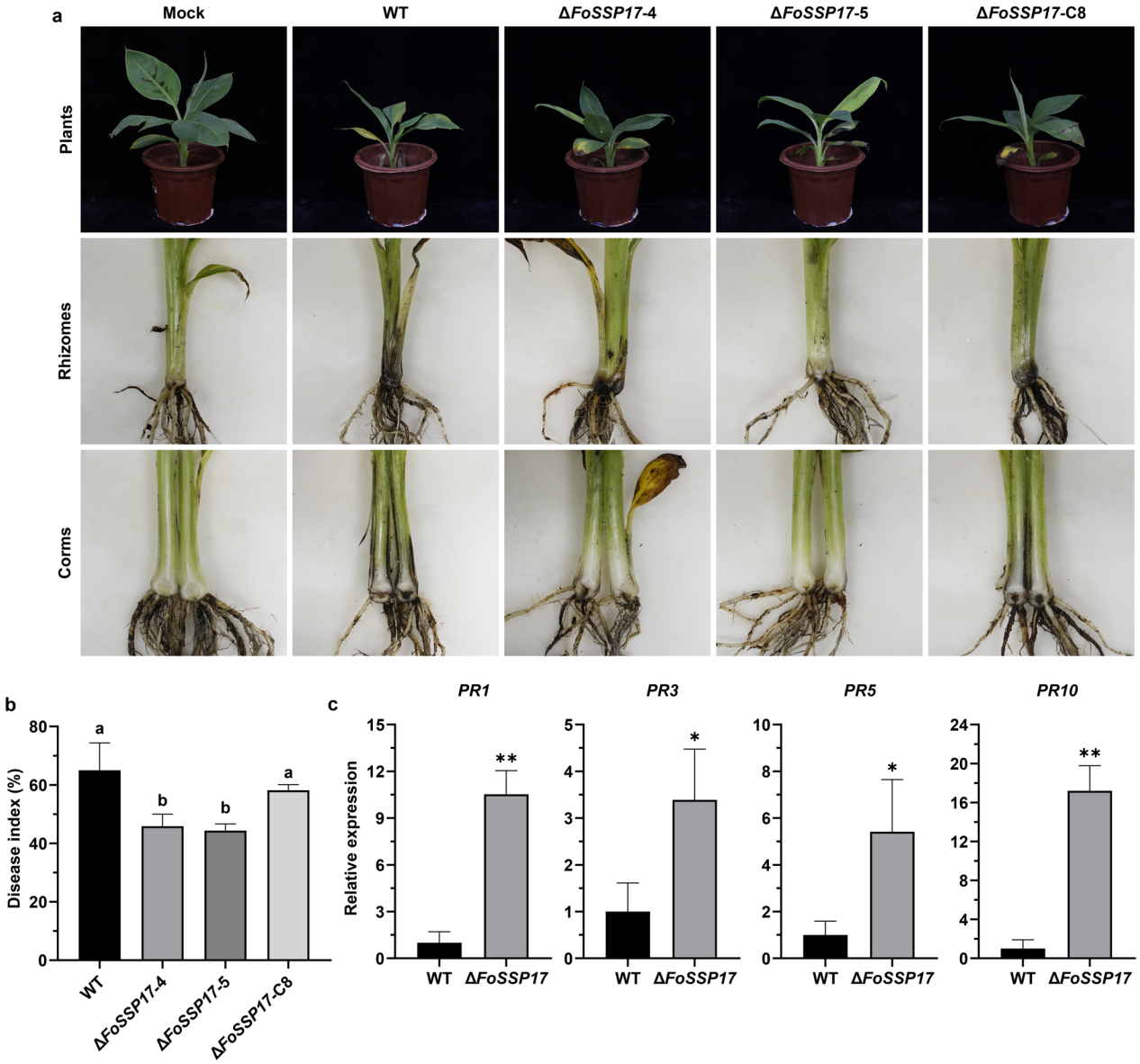

Fig. 6 The deletion of *FoSSP17* reduced the virulence of *Foc4* on banana and triggered host immune responses. **a** The 'Cavendish' bananas were inoculated with the conidia suspensions of different strains. Disease symptoms of plants, rhizomes, and corms infected with wild-type (WT), *FoSSP17* mutant (Δ*FoSSP17*-4 and Δ*FoSSP17*-5), and complemented (Δ*FoSSP17*-C8) stains are shown. Photographs were taken 30 dpi. **b** The disease index was calculated from banana plants infected with indicated *Foc* strains (30 dpi). **c** qRT-PCR assay of transcript levels of *PR* genes (*PR1*, *PR3*, *PR5* and *PR 10*). Total RNA was extracted 3 dpi from banana roots infected by WT and *FoSSP17* deletion mutants. The banana *Actin* gene was used as the internal reference gene. Relative expression of *PR* genes in WT calibrated to the levels of *Actin* was arbitrarily set to 1. For **b**, **c**, data shown are means ± SD calculated from three biological replicates. Statistical analyses were performed with One-way analysis of variance (ANOVA), Tukey's multiple comparisons test and Student's *t*-test. Different letters indicate significant differences ($P < 0.05$). *$P < 0.05$; **$P < 0.01$

in *N. benthamiana* leaves (Sun et al. 2022). We combined these methods in this study and set up a screening system to identify the CEs in *Foc4*. We identified 12 CEs capable of suppressing BAX-triggered PCD and being up-regulated during infection of banana plants. Further functional characterization of FoSSP17 demonstrates its virulence importance. Our work established an efficient effector-screening method and identified FoSSP17 as a novel virulence factor in *Foc4*.

Foc4 is a vascular pathogen belonging to *Fusarium oxysporum* (*Fo*), which could secrete small effectors called SIX proteins in the xylem. *Fusarium oxysporum* f. sp. *lycopersici* (*Fol*) secretes many SIX proteins to promote infection, and 14 SIX proteins were identified

(SIX1-14). Among all SIX proteins, the *SIX1* homolog gene deletion mutants in *Foc4* reduced the virulence, which is necessary for *I-3*-mediated resistance (Rep et al. 2004; Widinugraheni et al. 2018). SIX3 is an avirulence protein (Avr2) recognized by the *I-2* resistance gene (Houterman et al. 2009). However, many other effectors' functions are still unknown in *Foc*. In this study, we identified a novel protein FoSSP17 with a functional SP, and transient expression of FoSSP17 (with or without SP) in tobacco leaves suppressed BAX-triggered PCD (Fig. 3a). In addition, the virulence function of FoSSP17 was determined by banana root infection assay with targeted gene deletion and complementation in *Foc4*. Through subcellular localization experiment, we found that FoSSP17 localized in the nucleus and plasma membrane in *N. benthamiana* cells (Fig. 2b). To further ascertain the localization of FoSSP17, we used a functional SP from PR1 to drive the secretion of FoSSP17 and found that $FoSSP17^{SP(PR1)}$:eGFP localized in the nucleus and plasma membrane. Therefore, we speculate that the SP of PR1 might drive the secretion of FoSSP17:eGFP, which re-entered plant cells afterward. Interestingly, FoSSP17:eGFP, when transiently expressed, could aggregate as spots in the cytoplasm. However, the mechanism behind this phenomenon is still unclear and needs further investigation. In conclusion, these results indicate that FoSSP17 could function as a virulence factor of *Foc4* and might translocate inside host cells to exert its function.

Fo has a broad host range, but each formae speciale has a specialized host range (Edel-Hermann and Lecomte 2019). In other strains of *Fusarium oxysporum*, *SIX* genes have been proven to be related to host specificity (Williams et al. 2016). Recent studies show that the variation of host specificity is associated with some *SIX* genes. When non-pathogenic strains gain *SIX* genes, they will successfully infect the host and become a new pathogenic strain. Thus, *SIX* genes could be a marker gene to identify different host specialized forms (Jangir et al. 2021). In this study, we found that FoSSP17 is conserved across the *Fusarium* genus by phylogenetic analysis, and the amino acid identity in the *Fusarium* genus is higher than 57.31% (Fig. 1a). The homologs of FoSSP17 are similar between formae speciales, but obvious differences exist among different species, especially at N-terminus (Fig. 1b). In addition, previous studies demonstrated that SIX proteins are unique to *Fo*, except for SIX6, and the homologs of SIX6 have been found in *Colletotrichum* genus (Gawehns et al. 2014). Interestingly, akin to SIX proteins, most homologs of FoSSP17 distribute in the *Fusarium* genus, but some exist in other genus belonging to Hypocreomycetidae subclass including *Colletotrichum* genus. In the future, additional FoSSP17 homologs from other species will be tested to determine whether they have similar functions and are required for the virulence of pathogens.

PRRs at the cell surface recognize PAMPs or MAMPs when plants are infected by pathogens. The defense signaling pathways, including SA, JA, and ET, are subsequently activated, leading to the accumulation of PR proteins, which efficiently defend against the pathogen infection. For example, PR3 can function as a chitinase which degrades chitin, the main component of the fungal cell wall, and it had an inhibitory effect on *Tobacco mosaic virus* (TMV) infection (Šindelářová and Šindelář 2005). In this study, we found that infection of the *FoSSP17*-gene-deletion mutants led to an up-regulated expression of *PR* genes including *PR1*, *PR3*, *PR5,* and *PR 10* in banana plants (Fig. 6c). We speculate that FoSSP17 could suppress pattern-triggered immunity in plants. We transiently expressed FoSSP17 proteins in *N. benthamiana* leaves and found that FoSSP17 suppressed ROS accumulation and callose deposition elicited by flg22 (Fig. 4a–d). Moreover, FoSSP17 reduced the expression of *PR3*, *LOX*, and *ERF1* genes (Fig. 4e). The results suggested that FoSSP17 manipulates plant innate immunity by suppressing JA and ET-mediate signaling pathways. In the future, we will focus on finding the receptors or signaling targets of FoSSP17 in banana roots to investigate how FoSSP17 manipulates plant immunity and elucidate the underlying molecular mechanisms.

Conclusions

In this study, we set up a multi-step screening system (candidate effector prediction, RNA-seq-based expression level analysis, and cell death manipulative activity assessment based on transient expression in *N. benthamiana*) to identify candidate virulence-related effectors. We identified 12 CEs that suppressed BAX-triggered PCD and were up-regulated during banana infection. In addition, we revealed a novel conserved protein, FoSSP17, which is required for full virulence of *Foc* and suppresses pattern-triggered immunity in plants by decreasing ROS and callose accumulations. This study provides not only an efficient way to screen CEs but also insights into the pathogenic mechanisms of banana Fusarium wilt.

Methods

Fungal and bacterial strains and the growth of plants

The WT *Fusarium oxysporum* f. sp. *cubense* race 4 (*Foc4*) strain II5 (NRRL#54006) was grown on PDA medium at 25°C in the dark. The gene deletion mutants and complemented strains were cultured on PDA medium with 60 μg/mL hygromycin B or G418, respectively. *N. benthamiana* was grown in a growth room at 24°C (16 h/8 h, day/night). 'Cavendish' banana (AAA, Brazilian) plantlets with 5–6 leaves were grown in a greenhouse at 28 ± 2°C

(16 h/18 h, day/night). *Escherichia coli* (DH5a) and *A. tumefaciens* (GV3101) were stored at −80°C and cultured on lysogeny broth (LB) at 37°C and 28°C, respectively. The yeast strain YTK12 was cultured on yeast extract peptone dextrose (YEPD) medium at 30°C.

Bioinformatic analysis

The genome sequence of *Foc4* strain II5 (NRRL#54,006) was downloaded from NCBI (https://www.ncbi.nlm.nih.gov/Traces/wgs/?val=AGND00000000.1). The CEGs of *Foc4* were predicted based on a streamed pipeline (Additional file 1: Figure S1) with the following criteria: (1) having an SP sequence; (2) no transmembrane domain sequence; (3) the value of EffectorP over 0.59. The SP of protein was identified by SignalP 5.0 (https://services.healthtech.dtu.dk/service.php?SignalP-5.0) (Almagro Armenteros et al. 2019). The transmembrane domain of protein was identified using TMHMM 2.0 (https://services.healthtech.dtu.dk/service.php?TMHMM-2.0) (Krogh et al. 2001). The effector values of protein were determined by EffectorP 3.0 (https://effectorp.csiro.au/) (Sperschneider and Dodds 2022). The DNA sequence of FoSSP17 (FOIG_10239) was downloaded from NCBI (Genomic Sequence: NW_022158703.1). The sequences of FoSSP17 homologs were identified from NCBI NR and Ensemble Fungi database by BlastP search programs. The phylogenetic tree was constructed by MEGA11 using the maximum-likelihood method (Tamura et al. 2021). Clustal W was used for amino acid alignments, and GeneDoc was used for editing alignment results (Larkin et al. 2007).

RNA sequencing and transcriptome analysis

For RNA extraction and sequencing analysis, 15 samples (three independent samples for each sample type) were collected, including conidia (CON), hyphae (HYP), and the inoculated root (IR) of banana at different time points (24, 48, and 72 hpi). Total RNA was extracted, enriched, and reverse-transcribed into cDNA. Paired-end sequencing was performed using Illumina Novaseq6000 by Gene Denovo Biotechnology Co. (Guangzhou, China).

All paired-end clean reads were aligned against the reference genome (*Fusarium oxysporum* NRRL 54006, GCF_000260195.1) using HISAT2.2.4 (Kim et al. 2015). The value of fragment per kilobase of transcript per million mapped reads (FPKM) was calculated to quantify the transcript levels of the 15 samples by RSEM software (Li and Dewey 2011). The correlation analysis was performed by R. The correlation coefficient between two replicas was calculated to evaluate repeatability between samples. The closer the correlation coefficient gets to 1, the better the repeatability between two parallel experiments. Differential expression analysis was performed by DESeq2 and edgeR software. The genes with the false discovery rate (FDR) parameter below 0.05 and a fourfold-change threshold were considered DEGs.

RNA extraction and qRT-PCR assay

Total RNAs of infected banana roots or treated tobacco leaves were extracted using the Eastep R Super Total RNA Extraction Kit (Promega Biotech) following the manufacturer's instructions. First-strand complementary DNA (cDNA) was synthesized using the RevertAid First Stand cDNA Synthesis Kit (Thermo Fisher Scientific) following the manufacturer's protocol. Quantitative RT-PCR was performed using QuantStudio^{TM}5 Real-Time PCR Instrument with SuperReal PreMix Plus (TianGen Biotech) according to the manufacturer's protocol. The *Actin* (EMT65107.1) and *NbActin* (AFD62804.1) genes were used as reference genes for normalization. The gene transcript levels were analyzed with the comparative threshold cycle (Ct) method using QuantStudio$^{™}$ Design&Analysis Software v1.5.2. At least three biological replicates were performed.

Plasmid construction

The full-length coding sequences of 15 CEGs (the His-tag is fused at their N-termini) were amplified from the cDNA of *Foc4* and cloned into the pGR107 vector digested with specific enzymes (*Cla*I and *Sal*I) using T4 DNA Ligase (Takara Biotech). The coding sequence of *FoSSP17* with or without the SP was cloned into both pGR107-*GFP* and pBin-*eGFP* vectors digested with specific enzymes (*Cla*I for pGR107-*GFP* vector, *Kpn*I for pBin-*eGFP* vectors) using ClonExpress II One Step Cloning Kit (Vazyme Biotech). The coding sequence of FoSSP17$^{\Delta SP}$ with the SP of PR1 was cloned into the pBin-eGFP vectors digested with *Kpn*I using ClonExpress II One Step Cloning Kit (Vazyme Biotech). The coding sequence of SP from FoSSP17 was cloned into pSUC2 vectors digested with *EcoR*I and *Xho*I using ClonExpress II One Step Cloning Kit (Vazyme Biotech). To construct vector (pFL2-*FoSSP17*-C) for the complementation test, the encoding region and native promoter of *FoSSP17* were cloned into the *Xho*I site of the pFL2 vector containing the G418 resistance gene (Chen et al. 2014). All fragments were amplified using Phusion Plus DNA polymerase (Thermo Fisher Scientific). All constructs were validated by sequencing in Sangon (Sangon Biotech). All primers used in this study are listed in Additional file 2: Table S2.

Transient expression of proteins

N. benthamiana plants grown for 4–6 weeks were used for transient expression assays. For the cell death suppression assays, pGR107 or pGR107-*GFP* vectors

carrying the tested genes were transformed into *A. tumefaciens* GV3101. The resulting transformants were cultured in LB medium containing 50 μg/mg kanamycin and 25 μg/mg rifampicin at 28°C. The bacterial pellets were resuspended in infiltration buffer containing 10 mM $MgCl_2$, 5 mM 2-(N-morpholino) ethanesulfonic acid (MES, pH 5.6), and 150 μM acetosyringone (AS), and the concentration was adjusted to the OD_{600} of 0.6. After 2 h of incubation, the bacterial suspensions were infiltrated into tobacco leaves 24 h before infiltrating GV3101 bearing the BAX-expressing construct. The cell death results were photographed at 6 dpi. For subcellular localization assays, the GV3101 carrying pBin-*FoSSP17-eGFP*, pBin-*FoSSP17*$^{\Delta SP}$*-eGFP* or pBin-*FoSSP17*$^{SP(PR1)}$*-eGFP* vectors were resuspended in infiltration buffer at an OD_{600} of 0.01 and injected into plant leaves. The GFP fluorescence was observed at 36 hpi by confocal microscopy.

Measurement of electrolyte leakage

The electrolyte leakage of agroinfiltrated leaf zones was measured to quantify cell death as previously described (Yu et al. 2012), with slight modifications. Eight 9-mm leaf discs for each treatment from agroinfiltrated areas were taken at 5 dpi, and washed in distilled water. The clean leaf discs were pooled and transferred to a tube with 5 mL distilled water and incubated at room temperature for 6 h. The solutions were measured using a conductometer (DDB-12H, Zhejiang, China) to obtain the conductivity value A. Then, the leaf discs were boiled for 5 min and cooled to room temperature before measuring the conductivity again to get the value B. The relative electrolyte leakage is calculated as A/B × 100%. The experiments were repeated three times.

Signal peptide activity tests

The recombinant pSUC2-*FoSSP17*^{SP} vector was transformed into the yeast strain YTK12 and screened on CMD-W (a screening medium lacking tryptophan) medium. The positive colonies were successively replica-plated on YPRAA medium plates for verifying invertase secretion activity. The TTC was used to test further the secretion activity because TTC can be reduced by TPF (Yin et al. 2018). The yeast strains containing pSUC2-*Avr1b*, pSUC2-*Mg87*, and empty pSUC2 vector were used as positive, negative, and blank control, respectively.

Confocal microscopy

For subcellar localization assays, the GFP fluorescence of protein fusions was observed at 36 h after transient expression in five-week-old *N. benthamiana* plants and imaged using a confocal laser scanning microscope (Olympus microscope FV1000, Tokyo, Japan). An excitation wavelength of 488 nm and an emission wavelength of 505–530 nm were used to capture GFP fluorescence.

ROS accumulation and callose deposition assays

ROS accumulation and callose deposition were elicited with 20 μM flg22 (GenScript Inc, USA) in *N. benthamiana* leaves. To detect the ROS accumulation, tobacco leaves 48 h post agroinfiltration were stained with DAB staining solution containing 0.01% DAB and 0.01M phosphate buffer saline (PBS) for 12 h in the dark (Dong and Chen 2013). The tissues were cleared with 95% ethanol until the samples became transparent. For callose deposition assays, *N. benthamiana* leaves were rinsed in 95% ethanol until translucent and then immersed in aniline blue solution containing 0.05% aniline blue and 50 mM potassium phosphate buffer for 3 h in the dark (Herburger and Holzinger 2016), with slight modifications. All samples were imaged by microscopy (Olympus microscope TH4-200, Tokyo, Japan).

Protein extraction and western blot

Total *N. benthamiana* proteins were extracted with a Plant Total Protein Lysis Buffer (Sangon Biotech) according to the manufacturer's protocol. Denatured proteins were resolved on 12.5% sodium dodecyl sulfate–polyacrylamide gel electrophoresis (SDS-PAGE) and then transferred to 0.22 μm polyvinylidene difluoride (PVDF) membrane. Rabbit anti-GFP pAb and HRP Goat anti-rabbit IgG (Abclonal, Biotech) were used to detect the proteins on the PVDF membrane.

Gene deletion and complementation

We used a Split-marker approach to generate the *FoSSP17* gene deletion mutants in *Foc4*; the upstream and downstream sequences of FoSSP17 were fused with a partial fragment of HYG by overlapping PCR (Additional file 1: Figure S6a) (Goswami 2012). The fused fragments were purified using Gel Extraction Kit (Omega, Biotech) and transformed into the protoplasts of *Foc4* by PEG-mediated protoplast transformation. To generate genetically complemented strains, the purified pFL2-*FoSSP17*-C vectors were introduced into the protoplasts of the Δ*FoSSP17*-4 mutant strain using PEG-mediated transformation. All the mutations were verified by PCR and RT-PCR.

Morphology and virulence tests

For fungal growth assay, mycelial plugs 0.5 cm in diameter were inoculated on PDA plates and grown at 28°C. After 6 d, the colony diameter was measured, and photos were taken to examine the colony morphology. For each strain, 12 PDA plates were inoculated, and the

experiments were repeated three times. For fungal conidiation assay, five 9-mm mycelial plugs were cultured in 100 mL PDB medium and grown for 3 d in a shaker with 150 rpm under 28°C. The conidiation of different strains was calculated using a hemocytometer, and the experiments were performed three times.

For virulence assay, spores were collected from different strains cultured in PDB for 4–5 d. The conidia suspensions were adjusted to 10^7 conidia/mL and used to inoculate the clean roots of 'Cavendish' banana (Wang et al. 2022). These plantlets were transplanted into flowerpots and cultured in the same condition. The disease index of infected banana was evaluated at 30 dpi as described previously with some modifications: Disease index = ∑ (disease level × the number of associated banana plantlets)/(total banana plant number × highest disease level) × 100% (Zhang et al. 2019). Assays were repeated at least three times, and at least ten plants were inoculated with each strain in each assay.

Abbreviations

CEGs	Candidate effector genes
CEs	Candidate effectors
CON	Conidia
CWDEs	Cell wall degrading enzymes
DAB	Diaminobenzidine
DEGs	Differentially expressed genes
dpi	Days post-inoculation
ET	Ethylene
ETI	Effector-triggered immunity
ETS	Effector-triggered susceptibility
FAs	Fusaric acids
FDR	False discovery rate
Fo	*Fusarium oxysporum*
Foc	*Fusarium oxysporum* f.sp. *cubense*
Foc4	*Fusarium oxysporum* f.sp.*cubense* race 4
FPKM	Fragment per kilobase of transcript per million mapped reads
hpi	Hours post-inoculation
HR	Hypersensitive response
HYG	Hygromycin-resistance gene
HYP	Hyphae
IR	Inoculated root
JA	Jasmonic acid
MAMPs	Microbe-associated molecular patterns
NLR	Nucleotide-binding leucine-rich repeat
PAMPs	Pathogen-associated molecular patterns
PCD	Programmed cell death
PEG	Polyethylene glycol
PR	Pathogenesis-related
PRRs	Pattern recognition receptors
PTI	PAMP-triggered immunity
PVDF	Polyvinylidene difluoride
PVX	Potato virus X
qRT-PCR	Quantitative reverse transcription PCR
ROS	Reactive oxygen species
SA	Salicylic acid
SIX	Secreted in the xylem
SP	Signal peptide
TMD	Transmembrane domain
TMV	Tobacco mosaic virus
TPF	1,3,5-Triphenylformazan
TTC	2,3,5-Triphenyltetrazolium chloride
YSST	Yeast signal sequence trap

Supplementary Information

The online version contains supplementary material available at https://doi.org/10.1186/s42483-023-00198-6.

Additional file 1: Figure S1. Pipeline for *Foc4* candidate effector prediction. **Figure S2**. Identification of differently expressed genes. a Heatmap showing the relationships of the 15 RNA-seq datasets. Banana roots infected with *Foc4* 24, 48, and 72 h post-inoculation (IR24, 48, and 72). b Hierarchical clustering heatmap of differently expressed genes. **Figure S3**. Assay for suppression of BAX-triggered PCD in *N. benthamiana* by 12 CEs (FoSSP16, FoSSP17, FoSSP20, FoSSP25, FoSSP31, FoSSP40, FoSSP45, FoSSP48, FoSSP54, FoSSP55, FoSSP71, and FoSSP80). *N. benthamiana* leaves were co-infiltrated with *Agrobacterium tumefaciens* carrying each effector gene and *A. tumefaciens* carrying the BAX gene. Photos were taken 5 d after co-infiltration. The same results were obtained in three different assays of at least three biological replicates. **Figure S4**. qRT-PCR expressional profiles of 12 CEs during infection of banana roots. Total RNA of banana roots infected by *Foc4* was extracted. The sample of 0 h was collected from the strain grown on media, while those of 12, 24, 48, and 72 h were collected from inoculated banana roots at indicated time points after inoculation. The Actin gene of banana was used as the internal reference gene. Relative expression of CEs in 0 h was calibrated to the levels of *Actin* (set as 1). Data shown are means ± SD calculated from three biological replicates. The statistical analyses were performed with Student's *t*-test. *, $P < 0.05$; **, $P < 0.01$. **Figure S5**. Subcellular localization of FoSSP17SP(PR1):eGFP in N. benthamiana cells. a Confocal microscopy imaging of tobacco leaves with transiently expressing FoSSP17SP(PR1):eGFP fusion proteins. GFP was used as a control (Bars = 50 μm). b Western blot analysis of protein from tobacco leaves transiently expressing GFP and FoSSP17SP(PR1):eGFP. The same results were obtained in at least three biological replicates. **Figure S6**. Construction and identification of Δ*FoSSP17* and complementation mutants. **a** Schematic diagram of targeted gene replacement strategy. Small black arrows indicate primer binding sites, and large blue and red arrows indicate the target gene and HYG, respectively. **b** PCR validation of the deletion and complemented strains. *HYG* fragment was amplified with primers HYGF/HYGR (Lanes 1, 5, 9, 13); the upstream region of *FoSSP17* was amplified with 7F/HYR (Lanes 2, 6, 10, 14); the downstream region of *FoSSP17* was amplified with YGF/8R (Lanes 3, 7, 11, 15); the partial region of *FoSSP17* was amplified with 5F/FoSSP17CR (Lanes 4, 8, 12, 16). Lane M, DL4500 marker; Lane 17, water control.

Additional file 2: Table S1. Eighty candidate effector proteins of *Foc4* screened in this study. **Table S2**. Primers used in this study.

Acknowledgements

The authors thank Dr. Hongguang Cui at Hainan University for providing the pGR107 and pGR107-*GFP* plasmids and Dr. Xiao Li at Hainan University for providing the pBin-*eGFP* plasmids.

Author contributions

LZ, DC, and TW conceived and designed the study, jointly performed data analysis and wrote the manuscript. TW, YZ (Yang Zhao), and SL performed the experiments. TW, YX, and YZ (Yufang Zhang) analyzed data. LZ, DC, TW, XL, and ZK wrote and modified the manuscript. All authors read and approved the final manuscript.

Funding

This study was financially supported by Hainan Province Key R&D Project (No. ZDYF2022XDNY242), the National Natural Science Foundation of China (No. 32260648), the Scientific Research Foundation for Advanced Talents, Hainan University (No. KYQD(ZR)1873), the Hainan Provincial Natural Science Foundation of China (No. 320QN188), and the Scientific Research Foundation for Advanced Talents, Hainan University (No. KYQD(ZR)20027).

Availability of data and materials

The data that support the findings of this study are available from the corresponding author upon reasonable request.

Declarations

Ethical approval and consent to participate
Not applicable.

Consent for publication
Not applicable.

Competing interests
The authors declare that they have no competing interests.

Author details
[1]Hainan Yazhou Bay Seed Laboratory, Sanya Nanfan Research Institute of Hainan University, Sanya 572025, China. [2]Key Laboratory of Green Prevention and Control of Tropical Plant Diseases and Pests, Ministry of Education and School of Plant Protection, Hainan University, Haikou 570228, Hainan, China. [3]State Key Laboratory of Crop Stress Biology for Arid Areas and College of Plant Protection, Northwest A&F University, Yangling 712100, Shaanxi, China.

Received: 22 February 2023 Accepted: 28 August 2023
Published online: 08 September 2023

References

Ali S, Mir ZA, Tyagi A, Bhat JA, Chandrashekar N, Papolu PK, et al. Identification and comparative analysis of *Brassica juncea* pathogenesis-related genes in response to hormonal, biotic and abiotic stresses. Acta Physiol Plant. 2017;39(12):268. https://doi.org/10.1007/s11738-017-2565-8.

Ali S, Ganai BA, Kamili AN, Bhat AA, Mir ZA, Bhat JA, et al. Pathogenesis-related proteins and peptides as promising tools for engineering plants with multiple stress tolerance. Microbiol Res. 2018;212–213:29–37. https://doi.org/10.1016/j.micres.2018.04.008.

Almagro Armenteros JJ, Tsirigos KD, Sonderby CK, Petersen TN, Winther O, Brunak S, et al. SignalP 5.0 improves signal peptide predictions using deep neural networks. Nat Biotechnol. 2019;37(4):420–3. https://doi.org/10.1038/s41587-019-0036-z.

An B, Hou X, Guo Y, Zhao S, Luo H, He C, et al. The effector SIX8 is required for virulence of *Fusarium oxysporum* f.sp. cubense tropical race 4 to *Cavendish banana*. Fungal Biol. 2019;123(5):423–30. https://doi.org/10.1016/j.funbio.2019.03.001.

Asai S, Shirasu K. Plant cells under siege: plant immune system versus pathogen effectors. Curr Opin Plant Biol. 2015;28:1–8. https://doi.org/10.1016/j.pbi.2015.08.008.

Asai S, Yoshioka H. Nitric oxide as a partner of reactive oxygen species participates in disease resistance to necrotrophic pathogen *Botrytis cinerea* in *Nicotiana benthamiana*. Mol Plant Microbe in. 2009;22(6):619–29. https://doi.org/10.1094/mpmi-22-6-0619.

Ausubel FM. Are innate immune signaling pathways in plants and animals conserved? Nat Immunol. 2005;6(10):973–9. https://doi.org/10.1038/ni1253.

Boller T, Felix G. A renaissance of elicitors: perception of microbe-associated molecular patterns and danger signals by pattern-recognition receptors. Annu Rev Plant Biol. 2009;60:379–406. https://doi.org/10.1146/annurev.arplant.57.032905.105346.

Chen D, Wang Y, Zhou X, Wang Y, Xu JR. The Sch9 kinase regulates conidium size, stress responses, and pathogenesis in *Fusarium graminearum*. PLoS ONE. 2014;9(8):e105811. https://doi.org/10.1371/journal.pone.0105811.

Chisholm ST, Coaker G, Day B, Staskawicz BJ. Host-microbe interactions: shaping the evolution of the plant immune response. Cell. 2006;124(4):803–14. https://doi.org/10.1016/j.cell.2006.02.008.

Dita M, Barquero M, Heck D, Mizubuti ESG, Staver CP. Fusarium wilt of banana: current knowledge on epidemiology and research needs toward sustainable disease management. Front Plant Sci. 2018;9:1468. https://doi.org/10.3389/fpls.2018.01468.

Dong J, Chen W. The role of autophagy in chloroplast degradation and chlorophagy in immune defenses during *Pst* DC3000 (*AvrRps4*) infection. PLoS ONE. 2013;8:e73091. https://doi.org/10.1371/journal.pone.0073091.

Dubery IA, Sanabria NM, Huang JC. Nonself perception in plant innate immunity. Adv Exp Med Biol. 2012;738:79–107. https://doi.org/10.1007/978-1-4614-1680-7_6.

Edel-Hermann V, Lecomte C. Current status of *Fusarium oxysporum* formae speciales and races. Phytopathology. 2019;109(4):512–30. https://doi.org/10.1094/phyto-08-18-0320-rvw.

Gawehns F, Houterman PM, Ichou FA, Michielse CB, Hijdra M, Cornelissen BJC, et al. The *Fusarium oxysporum* effector Six6 contributes to virulence and suppresses I-2-mediated cell death. Mol Plant Microbe in. 2014;27(4):336–48. https://doi.org/10.1094/MPMI-11-13-0330-R.

Goswami RS. Targeted gene replacement in fungi using a split-marker approach. Methods Mol Biol. 2012;835:255–69. https://doi.org/10.1007/978-1-61779-501-5_16.

Guo L, Han L, Yang L, Zeng H, Fan D, Zhu Y, et al. Genome and transcriptome analysis of the fungal pathogen *Fusarium oxysporum* f. sp. *cubense* causing banana vascular wilt disease. PLoS ONE. 2014;9(4):e95543. https://doi.org/10.1371/journal.pone.0095543.

Gurdaswani V, Ghag SB, Ganapathi TR. FocSge1 in *Fusarium oxysporum* f. sp. *cubense* race 1 is essential for full virulence. BMC Microbiol. 2020;20(1):255. https://doi.org/10.1186/s12866-020-01936-y.

Herburger K, Holzinger A. Aniline blue and calcofluor white staining of callose and cellulose in the streptophyte green algae *Zygnema* and *Klebsormidium*. Bio-Protoc. 2016;6:e1969. https://doi.org/10.21769/bioprotoc.1969.

Houterman PM, Ma L, Van Ooijen G, De Vroomen MJ, Cornelissen BJC, Takken FLW, et al. The effector protein Avr2 of the xylem-colonizing fungus *Fusarium oxysporum* activates the tomato resistance protein I-2 intracellularly. Plant J. 2009;58(6):970–8. https://doi.org/10.1111/j.1365-313X.2009.03838.x.

Jamir Y, Guo M, Oh HS, Petnicki-Ocwieja T, Chen S, Tang X, et al. Identification of *Pseudomonas syringae* type III effectors that can suppress programmed cell death in plants and yeast. Plant J. 2004;37(4):554–65. https://doi.org/10.1046/j.1365-313x.2003.01982.x.

Jangir P, Mehra N, Sharma K, Singh N, Rani M, Kapoor R. Secreted in xylem genes: drivers of host adaptation in *Fusarium oxysporum*. Front Plant Sci. 2021;12:628611. https://doi.org/10.3389/fpls.2021.628611.

Jones JDG, Dangl JL. The plant immune system. Nature. 2006;444(7117):323–9. https://doi.org/10.1038/nature05286.

Jones JDG, Vance RE, Dangl JL. Intracellular innate immune surveillance devices in plants and animals. Science. 2016;354(6316):aaf6395. https://doi.org/10.1126/science.aaf6395.

Kamoun S, van West P, Vleeshouwers VGAA, de Groot KE, Govers F. Resistance of *Nicotiana benthamiana* to *Phytophthora infestans* is mediated by the recognition of the elicitor protein INF1. Plant Cell. 1998;10(9):1413–25. https://doi.org/10.1105/tpc.10.9.1413.

Kim D, Langmead B, Salzberg SL. HISAT: a fast spliced aligner with low memory requirements. Nat Methods. 2015;12(4):357–60. https://doi.org/10.1038/nmeth.3317.

Krijger JJ, Horbach R, Behr M, Schweizer P, Deising HB, Wirsel SG. The yeast signal sequence trap identifies secreted proteins of the hemibiotrophic corn pathogen *Colletotrichum graminicola*. Mol Plant Microbe in. 2008;21(10):1325–36. https://doi.org/10.1094/mpmi-21-10-1325.

Krogh A, Larsson B, von Heijne G, Sonnhammer EL. Predicting transmembrane protein topology with a hidden Markov model: application to complete genomes. J Mol Biol. 2001;305(3):567–80. https://doi.org/10.1006/jmbi.2000.4315.

Lacomme C, Santa CS. Bax-induced cell death in tobacco is similar to the hypersensitive response. Proc Natl Acad Sci USA. 1999;96(14):7956–61. https://doi.org/10.1073/pnas.96.14.7956.

Larkin MA, Blackshields G, Brown NP, Chenna R, McGettigan PA, McWilliam H, et al. Clustal W and Clustal X version 2.0. Bioinformatics. 2007;23(21):2947–8. https://doi.org/10.1093/bioinformatics/btm404.

Lei X, Lan X, Ye W, Liu Y, Song S, Lu J. *Plasmopara viticola* effector PvRXLR159 suppresses immune responses in *Nicotiana benthamiana*. Plant Signal Behav. 2019;14(12):1682220. https://doi.org/10.1080/15592324.2019.1682220.

Li B, Dewey CN. RSEM: accurate transcript quantification from RNA-Seq data with or without a reference genome. BMC Bioinformatics. 2011;12(1):323. https://doi.org/10.1186/1471-2105-12-323.

López-Díaz C, Rahjoo V, Sulyok M, Ghionna V, Martín-Vicente A, Capilla J, et al. Fusaric acid contributes to virulence of *Fusarium oxysporum* on plant and

mammalian hosts. Mol Plant Pathol. 2018;19(2):440–53. https://doi.org/10.1111/mpp.12536.
Meldrum RA, Fraser-Smith S, Tran-Nguyen LTT, Daly AM, Aitken EAB. Presence of putative pathogenicity genes in isolates of *Fusarium oxysporum* f. sp. *cubense* from Australia. Australas Plant Path. 2012;41:551–7. https://doi.org/10.1007/s13313-012-0122-x.
Newman MA, Sundelin T, Nielsen JT, Erbs G. MAMP (microbe-associated molecular pattern) triggered immunity in plants. Front Plant Sci. 2013;4:139. https://doi.org/10.3389/fpls.2013.00139.
Ploetz RC. Fusarium wilt of banana is caused by several pathogens referred to as *Fusarium oxysporum* f. sp. *cubense*. Phytopathology. 2006;96(6):653–6. https://doi.org/10.1094/phyto-96-0653.
Ploetz RC. Fusarium wilt of banana. Phytopathology. 2015a;105(12):1512–21. https://doi.org/10.1094/phyto-04-15-0101-rvw.
Ploetz RC. Management of fusarium wilt of banana: A review with special reference to tropical race 4. Crop Prot. 2015b;73:7–15. https://doi.org/10.1016/j.cropro.2015.01.007.
Rep M, van der Does HC, Meijer M, van Wijk R, Houterman PM, Dekker HL, et al. A small, cysteine-rich protein secreted by *Fusarium oxysporum* during colonization of xylem vessels is required for I-3-mediated resistance in tomato. Mol Microbiol. 2004;53(5):1373–83. https://doi.org/10.1111/j.1365-2958.2004.04177.x.
Saunders DG, Win J, Cano LM, Szabo LJ, Kamoun S, Raffaele S. Using hierarchical clustering of secreted protein families to classify and rank candidate effectors of rust fungi. PLoS ONE. 2012;7(1):e29847. https://doi.org/10.1371/journal.pone.0029847.
Shang S, Wang B, Zhang S, Liu G, Liang X, Zhang R, et al. A novel effector CfEC92 of *Colletotrichum fructicola* contributes to glomerella leaf spot virulence by suppressing plant defences at the early infection phase. Mol Plant Pathol. 2020;21(7):936–50. https://doi.org/10.1111/mpp.12940.
Šindelářová M, Šindelář L. Isolation of pathogenesis-related proteins from TMV-infected tobacco and their influence on infectivity of TMV. Plant Protect Sci. 2005;41(2):52–7. https://doi.org/10.17221/2747-pps.
Sperschneider J, Dodds PN. EffectorP 3.0: prediction of apoplastic and cytoplasmic effectors in fungi and oomycetes. Mol Plant Microbe Interact. 2022;35(2):146–56. https://doi.org/10.1094/mpmi-08-21-0201-r.
Sun X, Fang X, Wang D, Jones DA, Ma L. Transcriptome analysis of fusarium-tomato interaction based on an updated genome annotation of *Fusarium oxysporum* f. sp. lycopersici identifies novel effector candidates that suppress or induce cell death in *Nicotiana benthamiana*. J Fungi. 2022;8(7):672. https://doi.org/10.3390/jof8070672.
Tamura K, Stecher G, Kumar S. MEGA11: molecular evolutionary genetics analysis version 11. Mol Biol Evol. 2021;38(7):3022–7. https://doi.org/10.1093/molbev/msab120.
Wang Q, Han C, Ferreira AO, Yu X, Ye W, Tripathy S, et al. Transcriptional programming and functional interactions within the *Phytophthora sojae* RXLR effector repertoire. Plant Cell. 2011;23(6):2064–86. https://doi.org/10.1105/tpc.111.086082.
Wang Y, Zhang X, Wang T, Zhou S, Liang X, Xie C, et al. The small secreted protein FoSsp1 elicits plant defenses and negatively regulates pathogenesis in *Fusarium oxysporum* f. sp. cubense (Foc4). Front Plant Sci. 2022;13:873451. https://doi.org/10.3389/fpls.2022.873451.
Widinugraheni S, Niño-Sánchez J, van der Does HC, van Dam P, García-Bastidas FA, Subandiyah S, et al. A SIX1 homolog in *Fusarium oxysporum* f.sp. *cubense* tropical race 4 contributes to virulence towards *Cavendish banana*. PLoS ONE. 2018;13(10):e0205896. https://doi.org/10.1371/journal.pone.0205896.
Williams AH, Sharma M, Thatcher LF, Azam S, Hane JK, Sperschneider J, et al. Comparative genomics and prediction of conditionally dispensable sequences in legume-infecting *Fusarium oxysporum* formae speciales facilitates identification of candidate effectors. BMC Genomics. 2016;17:191. https://doi.org/10.1186/s12864-016-2486-8.
Xiang J, Li X, Wu J, Yin L, Zhang Y, Lu J. Studying the mechanism of *Plasmopara viticola* RxLR effectors on suppressing plant immunity. Front Microbiol. 2016;7:709. https://doi.org/10.3389/fmicb.2016.00709.
Yin W, Dong S, Zhai L, Lin Y, Zheng X, Wang Y. The *Phytophthora sojae* Avr1d gene encodes an RxLR-dEER effector with presence and absence polymorphisms among pathogen strains. Mol Plant Microbe in. 2013;26(8):958–68. https://doi.org/10.1094/mpmi-02-13-0035-r.
Yin W, Wang Y, Chen T, Lin Y, Luo C. Functional evaluation of the signal peptides of secreted proteins. Bio-Protoc. 2018;8(9):e2839. https://doi.org/10.21769/bioprotoc.2839.
Yu X, Tang J, Wang Q, Ye W, Tao K, Duan S, et al. The RxLR effector Avh241 from *Phytophthora sojae* requires plasma membrane localization to induce plant cell death. New Phytol. 2012;196(1):247–60. https://doi.org/10.1111/j.1469-8137.2012.04241.x.
Zhang L, Cenci A, Rouard M, Zhang D, Wang Y, Tang W, et al. Transcriptomic analysis of resistant and susceptible banana corms in response to infection by *Fusarium oxysporum* f. sp. *cubense* tropical race 4. Sci Rep. 2019;9(1):8199. https://doi.org/10.1038/s41598-019-44637-x.
Zhang X, Huang H, Wu B, Xie J, Viljoen A, Wang W, et al. The M35 metalloprotease effector FocM35_1 is required for full virulence of *Fusarium oxysporum* f. sp. *cubense* tropical race 4. Pathogens. 2021;10(6):670. https://doi.org/10.3390/pathogens10060670.
Zhang L, Yan J, Fu Z, Shi W, Ninkuu V, Li G, et al. FoEG1, a secreted glycoside hydrolase family 12 protein from *Fusarium oxysporum*, triggers cell death and modulates plant immunity. Mol Plant Pathol. 2021;22:522–38. https://doi.org/10.1111/mpp.13041.
Zhou JM, Zhang Y. Plant immunity: danger perception and signaling. Cell. 2020;181(5):978–89. https://doi.org/10.1016/j.cell.2020.04.028.